Heliyon

ELSEVIER

Received:
29 October 2018
Revised:
25 March 2019
Accepted:
8 April 2019

Cite as: Barnabás Horváth, Melinda Rigó, Sándor Guba, István Szalai, Réka Barabás. Magnetic field response of aqueous hydroxyapatite based magnetic suspensions. Heliyon 5 (2019) e01507. doi: 10.1016/j.heliyon.2019.e01507

Magnetic field response of aqueous hydroxyapatite based magnetic suspensions

Barnabás Horváth [a,*], **Melinda Rigó** [b], **Sándor Guba** [a], **István Szalai** [a,c], **Réka Barabás** [b]

[a] *Institute of Physics and Mechatronics, University of Pannonia, 10 Egyetem St, H-8200 Veszprém, Hungary*

[b] *Department of Chemistry and Chemical Engineering of the Hungarian Line of Study, Faculty of Chemistry and Chemical Engineering, Babeş-Bolyai University, 11 Arany Janos St, RO-400028 Cluj-Napoca, Romania*

[c] *Institute of Mechatronics Engineering and Research, University of Pannonia, 18/A Gasparich Márk St, H-8900 Zalaegerszeg, Hungary*

* Corresponding author.
E-mail address: bhorvath@almos.uni-pannon.hu (B. Horváth).

Abstract

During the biomedical and biotechnological applications of hydroxyapatite based magnetic biomaterials the response to various magnetic fields (i.e. change in flow behavior) plays a pivotal role in manipulating these materials. Numerous studies discuss the synthesis, characterization and possible applications of magnetic hydroxyapatite, however the number of reports related to the magnetic response is limited. In this study we investigated the response of aqueous suspensions of magnetite/hydroxyapatite composites with gelatin as an additive to homogeneous and inhomogeneous magnetic fields. Under homogeneous field the change in rheological properties was determined, and correlated with the composition of the composites. The effect of magnetite and gelatin content on the zero field viscosity and magnetic susceptibility were also evaluated. The response to inhomogeneous field was characterized by measuring the magnetic body force acting on droplets of the aqueous suspensions. We found that the formulation of the composites and the presence of additive largely affect the magnetic response.

Keywords: Materials Science, Materials Chemistry

https://doi.org/10.1016/j.heliyon.2019.e01507

1. Introduction

Magnetic field-responsive materials are widely used in biotechnology and for various biomedical applications including targeted drug delivery, magnetic resonance imaging (MRI), hyperthermia-based cancer treatments, cell labeling and separation, tissue engineering [1, 2, 3]. Mostly these multifunctional materials are composed of a magnetic (e.g. iron oxide) core and the necessary biocompatibility and further functionality are provided by additional components [4].

Magnetite (Fe_3O_4) and hydroxyapatite (HAp) composites display a combined effect of magnetic properties and excellent bioactivity, biocompatibility owing to HAp [5, 6]. The similar chemical composition of HAp to the inorganic component of natural bone makes these composites especially suitable for targeting bone tissue. Magnetic HAp composites are promising biomaterials for tissue engineering applications, where they are used directly as bone grafts, fillers, and scaffolds [7]. Furthermore, as drug delivery systems they have high efficiency, high drug loading capacity and enhanced precisions due to magnetic guidance [8]. The performance of these materials can be further tailored with additives, like natural biopolymers (e.g. gelatin) [9, 10].

Magnetic suspensions respond to, and are manipulated by external magnetic stimuli. The response to static magnetic field differs whether it is homogeneous or inhomogeneous. If the field is homogeneous (uniform in direction and magnitude) microstructural changes (e.g. agglomeration of the particles into chains, columns) occur in the material, which have significant impact on rheological and other macroscopic properties. Under inhomogeneous field (where the field gradient is non-zero) besides the microstructural changes a magnetic body force is acting throughout the volume of a magnetic suspension pointing in the direction of the field gradient. These phenomena are the basis for manipulating these materials and determine the physical interaction between the material and biological tissues [11]. During the applications of magnetic suspensions the change in flow behavior due to the external field and the zero field rheological properties which affect the handling, workability and injectability play a pivotal role [12, 13]. In order to formulate magnetic HAp suspensions with optimal rheological properties further important questions are how the magnetic response is influenced by the basic composition and the presence of additives. There are many papers discussing the synthesis, characterization and possible applications of magnetic HAp suspensions [14, 15, 16], but studies where the magnetic response (i.e. magnetorheology) is assessed are rather scarce.

In this study we investigated the behavior of aqueous suspensions of magnetite/hydroxyapatite (MHAp) composites in homogeneous and inhomogeneous magnetic fields. Composites with different magnetite content and with gelatin as an additive were synthesized and characterized. Our effort was focused on to study the magnetic

 https://doi.org/10.1016/j.heliyon.2019.e01507

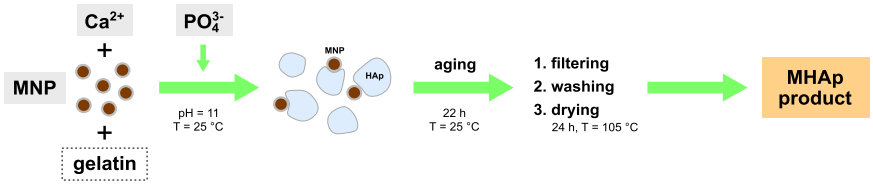

Figure 1. Synthesis of the MHAp composites via chemical precipitation method.

response in various fields, and how it is affected by the composition of the composites. The effect of magnetite concentration and gelatin content on the rheological properties in the absence and in the presence of a homogeneous magnetic field is discussed. Furthermore, the response of these suspensions to inhomogeneous field and the dependence of the arising magnetic force on the composition is addressed.

2. Experimental

2.1. Materials and synthesis

The magnetite/hydroxyapatite composites were prepared in two steps. First, magnetite nanoparticles in aqueous medium were synthesized separately by Aqueous Colloids Research Group, University of Szeged with co-precipitation method [17]. The average diameter of the magnetite nanoparticles is ≈10 nm, and they are coated with PAM (poly(acrylic acid-co-maleic acid)) polyelectrolyte to stabilize the aqueous colloid. The magnetite concentration was 5.19 wt%. The second step during the preparation of the MHAp composites was the precipitation of HAp (Figure 1). As precursors solutions of calcium nitrate ($Ca(NO_3)_2 \cdot 4H_2O$) (Reanal, Hungary) and diammonium hydrogen phosphate ($(NH_4)_2HPO_4$) (Merck, Germany) were prepared in distilled water separately, with the desired Ca/P = 1.67 ratio of stoichiometric HAp. Specific volume of the colloid of magnetite nanoparticles (and gelatin (Reanal, Hungary) in the case of composites with additive) were added to the $Ca(NO_3)_2$, and the pH was adjusted to 11 with ammonia solution. The diammonium hydrogen phosphate solution was added dropwise to the mixture during continuous stirring. The resulting precipitate was further stirred and aged for 22 h at room temperature and under atmospheric pressure. The precipitate was filtered and washed with distilled water, and dried at 105 °C for 24 hours. The final product was crushed into powder in an agate mortar. MHAp composites with different magnetite content were synthesized and the gelatin containing variants (MHApG) were also prepared. The exact compositions (c_M magnetite and c_G gelatin concentration) are summarized in Table 1.

https://doi.org/10.1016/j.heliyon.2019.e01507

2.2. Suspension preparation

Mechanical grinding was applied to reduce the size of the aggregates in the composites. The powders were ground for 4 h in a high speed micro mill (Retsch, Germany) with agate mortar and pestle. All suspensions were prepared by mixing the ground powders with distilled water. The solid loading of the aqueous suspensions was 25.0 wt% in all cases. After vigorous stirring the suspensions were placed in an Emmi-5 ultrasonic bath (EMAG, Germany) for 30 minutes to further homogenize the samples.

2.3. Characterization

The microstructure and morphology of the composites were examined by transmission electron microscopy (TEM) with an H-7650 instrument (Hitachi, Japan). Particle size, powder morphology, and chemical elemental composition analysis were done by scanning electron microscopy coupled with energy-dispersive X-ray spectroscopy (SEM/EDS). An Apreo SEM (Thermo Fisher, USA) equipped with Octane Elect EDS (AMETEK, USA) was used at 20.0 kV.

The infrared spectra of the solid composites were recorded on a Spectrum Two FT-IR spectrometer (Perkin-Elmer, USA) in ATR (attenuated total reflection) mode in the 4000 to 400 cm^{-1} range with 512 scans.

The specific surface area (SSA) and the average pore size diameter of the synthesized composites were determined by the Brunauer-Emmett-Teller (BET) and the Barrett-Joyner-Halenda (BJH) method using nitrogen adsorption/desorption isotherms recorded with an ASAP 2000 equipment (Micromeritics, USA). Before the measurements the samples were degassed at 160 °C under vacuum ($p \leq 1.3$ Pa).

The magnetic properties of the suspensions were characterized by magnetic susceptibility measurements. The ac susceptibility of the samples was measured by inductance method with an Agilent 4284A impedance analyzer between $f = 20$ Hz and 100 kHz. The intensity of the ac measuring field was low enough not to cause any structural change in the suspensions. The data were extrapolated to 0 Hz in order to obtain the static initial susceptibility (χ_0). The susceptibility was measured with an error of ± 0.001.

The magnetic force acting on droplets of the aqueous MHAp suspensions in an inhomogeneous magnetic field was measured with a custom built setup [18]. A disk-shaped silicone rubber sample holder ($V = 0.073$ cm^3) was filled with MHAp suspension and placed between the asymmetric (planar and conical) iron poles of an electromagnet (VEB Polytechnik, Phylatex, Germany). The coil was driven by a Hewlett-Packard 6030A power supply at a maximum of 3 A coil current. The

 https://doi.org/10.1016/j.heliyon.2019.e01507

average magnetic field strength was adjusted in the range of 120-238 kA/m, while the corresponding gradient was between 2821 and 22089 kA/m^2. The force exerted on the material was determined by measuring the weight increase with a KERN PLS 1200 3A analytical balance. The error of the force measurement was 0.02 mN.

The rheological measurements with and without an external magnetic field were conducted using a Physica MCR 301 rotational rheometer (Anton Paar, Austria) equipped with an MRD 70/1T magnetorheological (MR) accessory. Steady shear strain was applied to the suspensions in parallel plate geometry. The diameter of the rotating plate was 20 mm, and the gap between the plates was set to 1 mm. Viscosity curves of apparent viscosity (η) vs. shear rate ($\dot{\gamma}$) and flow curves of shear stress (τ) vs. shear rate were obtained in an upward shear rate ramp in the 1-1000 s^{-1} range. Before each shear rate step a sufficient length of time was waited to reach a steady state. The time dependence of the viscosity was measured at a constant $\dot{\gamma} = 10\ s^{-1}$ shear rate. Before all rheological tests the samples were pre-sheared for 60 s at $\dot{\gamma} = 10\ s^{-1}$ to develop a defined state. The external magnetic field generated by the MR accessory was perpendicular to the shear flow. It was switched on after the pre-shear and the magnetic induction was held at a constant $B = 791$ mT value. The temperature of the samples was regulated by circulating thermal fluid through the MRD 70/1T with a CC-K6 thermostat (Huber, Germany). All rheological tests were done at 25.0±0.1 °C. For these measurements we used freshly prepared suspensions, and the samples were loaded to the rheometer right after the ultrasonic homogenization.

3. Results and discussion

3.1. MHAp structure and morphology

The elemental analysis of the composites is shown in Figure 2. According to the EDS spectra the Ca/P ratio is between 1.55 and 1.66 which is consistent with slightly Ca deficient HAp [19]. Besides the main constituents the presence of iron can be confirmed, which indicates that the magnetite nanoparticles are attached to HAp. The elemental mapping images show that the HAp phase and the Fe oxide are homogeneously dispersed.

The infrared spectra of all synthesized MHAp and MHApG composites show the major characteristic bands of HAp. Intensive absorption peaks of phosphate group appear at 1090, 1026, and 964 cm^{-1} (asymmetrical and symmetrical stretching mode). The typical double band at 601 and 561 cm^{-1} and the peak at 473 cm^{-1} are also attributed to the vibrations of PO_4^{3-}. The OH^- group peaks are observed at 630 and 3562 cm^{-1} characteristic to the HAp phase [20]. The wide band from 3100 to 3600 cm^{-1} signals the presence of adsorbed water in all of the samples.

https://doi.org/10.1016/j.heliyon.2019.e01507

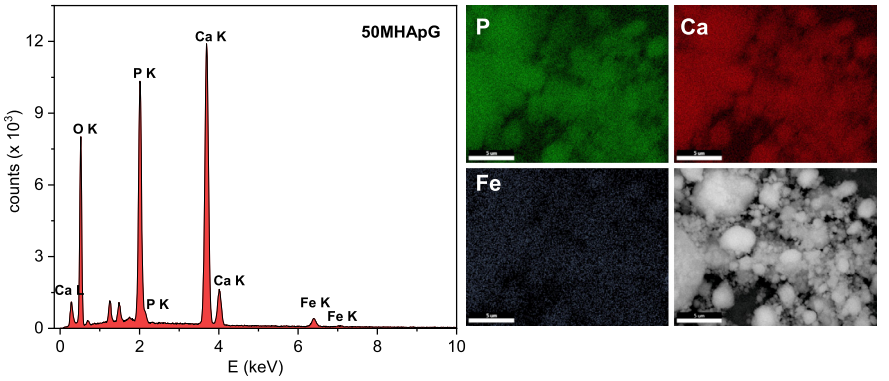

Figure 2. Representative EDS spectrum (left) and elemental mapping (right) of 50MHApG composite with gelatin additive and 3.57 wt% magnetite content.

Infrared absorption of magnetite occurs at 570 cm^{-1} (Fe-O vibration) and weakly at 1060 cm^{-1} (surface Fe-OH groups) [5], but in the IR spectra of the composites these bands are merged with the much more intense phosphate bands. The absorption peak at 1418 cm^{-1} together with the 874 cm^{-1} peak indicate the presence of CO_3^{2-} groups in the samples. This is typical for the wet precipitation method, when atmospheric CO_2 is dissolved in the reagents during the synthesis (especially due to the alkaline environment) [21]. The carbonate substitution suggests that the crystallization degree is low, similar to the structure of biological HAp. Comparing the spectra of the composites with and without gelatin it can be seen that peaks at 1241 and 1544 cm^{-1} appear, and the intensity of the 1642 cm^{-1} band increases in the MHApG samples. These bands correspond to the amide bands [22], which confirms the presence of gelatin in the MHApG composites.

The microstructure of the synthesized composites was characterized with TEM and representative images are shown in Figure 3. Both the MHAp (Figure 3a) and MHApG (Figure 3b) composites are agglomerates of 20-30 nm sized smaller nanoparticles. These particles have an irregularly shaped quasi spherical morphology. This is often the case when HAp is synthesized at high (>10) pH [23]. According to SEM images the shape of the clusters is irregular and the size distribution is highly non-uniform. The agglomerates are between 0.1 and 20 μm. The gelatin containing MHApG composites have a higher degree of agglomeration, and the surface of the clusters is smoother compared to MHAp composites.

The specific surface area of the composite powders determined with the BET method is presented in Table 1. The average pore size (D_{avg}) calculated according to the BJH method is also given. The porosity analysis shows that all composites are mesoporous materials with an average pore size in the range of 9.6-12.2 nm. The SSA of the MHAp is between 119-162 m^2/g which can be considered fairly large. The MHApG samples have a much lower SSA than the ones without gelatin at the same Fe_3O_4 content (48 vs. 125 m^2/g in the case of 10MHApG and 10MHAp, respectively).

https://doi.org/10.1016/j.heliyon.2019.e01507

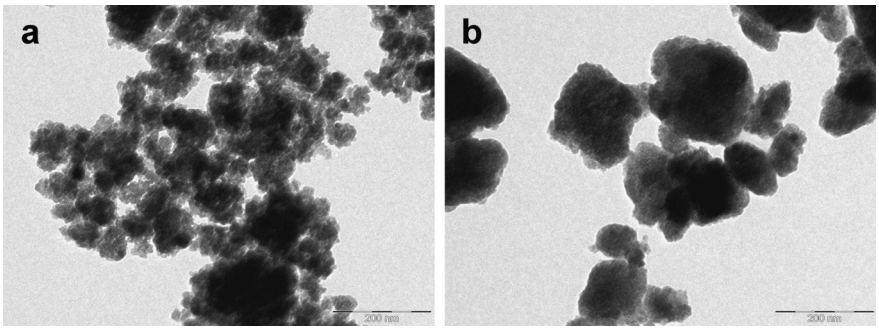

Figure 3. Representative TEM images of the 50MHAp (a) and the gelatin containing 50MHApG (b) composites. A difference in the particle size distribution can be observed.

Table 1. The composition, the specific surface area, the average pore size of the composites, and the dc magnetic susceptibility of the corresponding suspensions.

Composites	10MHAp	10MHApG	30MHAp	30MHApG	50MHAp	50MHApG
c_M (wt%)	0.57	0.57	2.17	1.70	4.93	3.57
c_G (wt%)	–	22.1	–	12.6	–	27.6
SSA (m^2/g)	125	48	162	108	119	38
D_{avg} (nm)	12.2	10.3	11.9	9.6	10.9	11.9
χ_0	0.003	0.004	0.013	0.010	0.032	0.028

The decrease of SSA is attributed to the higher degree of agglomeration, which is consistent with the morphological observations in the TEM images. Thus the presence of gelatin greatly decreases the SSA due to agglomeration, but there is no correlation between the magnetite concentration and the SSA.

3.2. Magnetic properties of MHAp suspensions

Both the MHAp and MHApG suspensions exhibited paramagnetic properties, with initial dc susceptibility between 0.003 and 0.032 (Table 1). A linear increase of χ_0 was observed with the magnetite loading of the MHAp and MHApG suspensions. However, above 3 wt% magnetite concentration the susceptibility increase was larger with the addition of gelatin compared to the χ_0 expected from only the magnetite concentration increase. Gelatin changes the interaction between the particles in suspension and hinders agglomeration (as it can be seen from the rheological results, see discussion below) and the resulting difference in particle size distribution could be responsible for the deviation in the measured susceptibility.

3.3. MHAp suspensions in external magnetic fields

Below we discuss the effect of homogeneous magnetic field on the rheological behavior of suspensions of the synthesized MHAp composites, and the magnetic

https://doi.org/10.1016/j.heliyon.2019.e01507

response to inhomogeneous field, which was characterized by measuring the arising magnetic body force.

3.3.1. Homogeneous magnetic field

Steady state shear flow behavior of the MHAp suspensions was determined in the presence and in the absence of external magnetic field. The investigation was limited to shear flow, because this is the dominant component of the flow during most applications. The behavior was characterized based on the viscosity and flow curves and the time dependence of the viscosity at constant shear rate. The shear rate regime was chosen to cover the range relevant for typical practical processes.

Shear rate dependence

First we discuss the shear rate dependence of the viscosity if the field strength is zero. The viscosity and flow curves of the suspensions with different magnetite and gelatin content without magnetic field is shown in Figure 4. There is a significant difference between the behavior of MHAp and MHApG suspensions. The MHAp samples show apparent yield stress (τ_y) and shear thinning within the investigated shear rate range, while with the addition of gelatin the behavior changes to almost Newtonian fluid, and no yield stress can be observed. The shear thinning of the MHAp samples is characteristic to particle suspensions [24] and it is the result of the agglomeration of the particles. If the fluid is quiescent or the shear rate is low and there is a net attractive potential between the particles, then they agglomerate into a 3D network that percolates the suspension volume. In the absence of a magnetic field the agglomeration is driven by the Van der Waals attraction force between the MHAp particles. This network of agglomerated particles is responsible for the apparent yield stress and the increased viscosity ($\eta \approx$ 1-10 Pa s) of the MHAp suspensions at low shear (compared to MHApG). The yield stress was estimated by extrapolating the flow curve back to zero shear rate. For the extrapolation the Seo-Seo model [25] was used, which fitted the experimental data well. The zero field yield stress of the MHAp suspensions varied between 1.47 and 23.58 Pa. After the suspension begins to flow and the shear rate is increased the particle network is broken down by shear forces. Thus, with increasing $\dot{\gamma}$ the size of the agglomerates is continuously decreasing, and this results in a reduction of the viscosity. At high shear rates the viscosity can reach a constant value, where the size of the clusters cannot be reduced only by shear forces.

The magnetite content has an effect on the rheological properties of the MHAp suspensions. With increasing Fe_3O_4 concentration there is a large decrease in viscosity, but the shear thinning character of the viscosity curves remain. The composites with more magnetite (30MHAp and 50MHap) show a Newtonian regime

 https://doi.org/10.1016/j.heliyon.2019.e01507

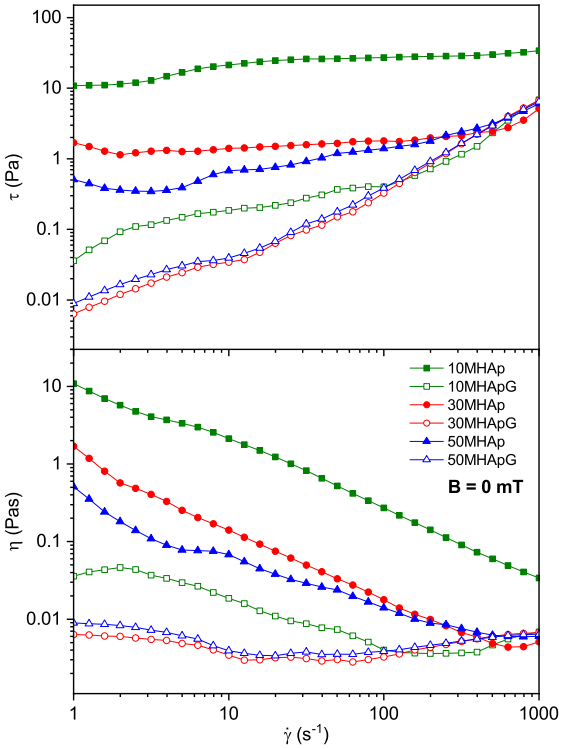

Figure 4. Flow curves (top) and viscosity curves (bottom) of the suspensions in the absence of magnetic field. The shear thinning behavior of the MHAp suspensions (filled symbols) changes to almost Newtonian with the addition of gelatin (empty symbols).

of $\eta \approx 0.006$ Pa s at high shear rates ($\dot{\gamma} > 500$ s^{-1}). Figure 5 shows the effect of the increased magnetite concentration, where the decrease in viscosity at small shear rate ($\dot{\gamma} = 10$ s^{-1}) can be seen. The estimated yield stress also decreases from 23.58 Pa to a value of 1.47 Pa as the magnetite concentration is increased to 4.93 wt%. This rheological behavior indicates that there is a net attraction potential between the particles, but with increasing magnetite content it becomes weaker.

Contrary to the MHAp samples, the gelatin containing MHApG suspensions behave almost like Newtonian fluids and have a much lower, but near constant viscosity ($\eta \approx$ 0.006 Pa s) through the shear rate ramp. Out of these composites the 10MHApG with the lowest magnetite content exhibited weak shear thinning in the lower shear rate regime, but reached the $\eta \approx 0.006$ Pa s Newtonian plateau after $\dot{\gamma} > 100$ s^{-1}. The addition of gelatin to the composites drastically lowers the viscosity of the suspensions. At small shear rates ($\dot{\gamma} = 10$ s^{-1}) this decrement in viscosity is around two orders of magnitude (Figure 5). For example, while the viscosity of 10MHAp suspension is $\eta = 2.127$ Pa s at $\dot{\gamma} = 10$ s^{-1}, then the corresponding 10MHApG suspension has a value of $\eta = 0.018$ Pa s. Gelatin – like many proteins – is a natural surfactant due to their amphiphilic and flexible nature. The bonded gelatin on the surface of the MHApG composites acts as a surfactant layer. The attractive

 https://doi.org/10.1016/j.heliyon.2019.e01507

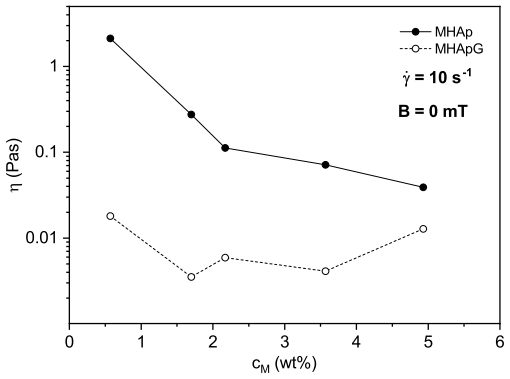

Figure 5. The zero field viscosity of the MHAp (filled symbols) and the gelatin containing MHApG (empty symbols) suspensions at $\dot{\gamma} = 10\ s^{-1}$ as a function of the magnetite concentration.

interaction between the particles is compensated by the electrostatic repulsion and the steric interaction of the gelatin covered particle surfaces and the net interparticle potential becomes repulsive [26]. This electrosteric barrier prevents agglomeration, therefore no attractive particle network can be formed, which results in the observed low viscosity. Unlike the MHAp suspensions, in the case of the MHApG samples the viscosity is almost independent of the magnetite concentration, as it is shown in Figure 5.

In a magnetic field a change of flow behavior was observed for all suspensions. As an example (50MHAp and 50MHApG) a comparison between zero field and $B = 791$ mT viscosity curves is given in Figure 6. In magnetic field the MHAp suspensions showed the previously observed shear thinning, while the MHApG samples retained the close to Newtonian flow behavior. As expected in magnetic field the estimated yield stress of the MHAp suspensions increased. For the MHApG suspensions no yield stress was observed despite the high intensity magnetic field, but the viscosity was greater than the corresponding zero field viscosity. Only the 50MHApG suspension with the highest magnetite loading showed a weak shear thinning regime in the 4-400 s^{-1} shear rate range. Figure 7 summarizes the $\Delta\eta$ viscosity increase of the suspensions in magnetic field at $\dot{\gamma} = 10\ s^{-1}$ shear rate. The values of viscosity increase are rather small ($\Delta\eta < 0.160$ Pa s), which is understandable for the relatively small (maximum 4.93 wt%) magnetite loading.

The particle aggregates of the composite have a permanent magnetic dipole moment because of the single domain magnetite nanoparticles. Furthermore, in an external magnetic field a magnetic dipole moment is also induced due to the magnetic permeability difference between the particles and the dispersion medium. Dipole-dipole interaction appear between the particles with magnetic moment, so the attraction force is increased in a magnetic field, and chain like structures are formed parallel with the field. Because of this attractive structure perpendicular to the shear flow the suspensions have a larger viscosity in a magnetic field. Figure 7 shows

 https://doi.org/10.1016/j.heliyon.2019.e01507

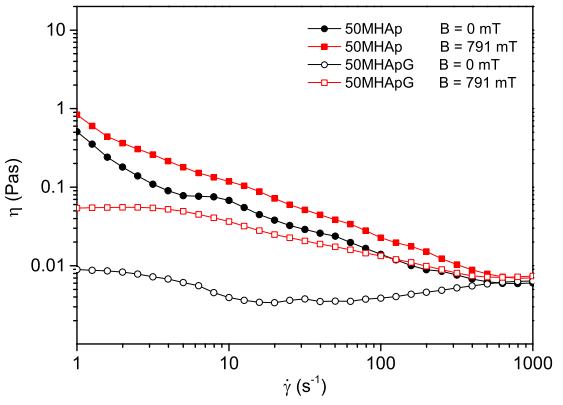

Figure 6. Viscosity curves of the 50MHAp (filled symbols) and 50MHApG (empty symbols) suspensions in the presence (rectangles) and in the absence (circles) of a magnetic field.

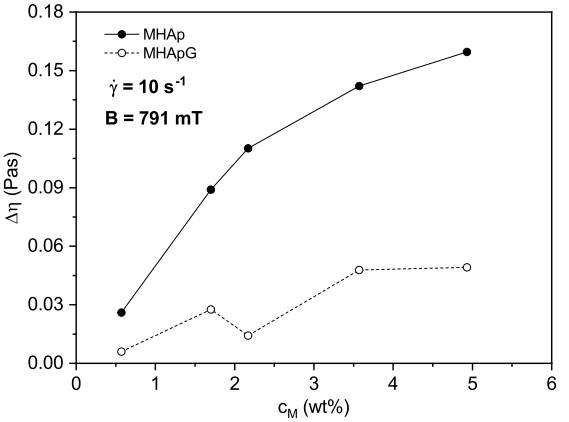

Figure 7. The change in viscosity of the MHAp (filled symbols) and the gelatin containing MHApG (empty symbols) suspensions in a magnetic field (B = 791 mT) as a function of the magnetite concentration.

how the magnitude of $\Delta\eta$ is influenced by the composition. On the one hand, as the composites have a higher magnetite loading the value of $\Delta\eta$ is increasing due to the stronger dipole-dipole interaction. This is true for the MHAp and the MHApG suspensions too. Depending on the magnetite concentration the $\Delta\eta$ of the MHAp suspensions is between 0.026 and 0.160 Pa s. On the other hand the absolute viscosity increase is much smaller if the composites contain gelatin. The $\Delta\eta$ of MHApG samples is increasing only from 0.006 to 0.049 Pa s. Therefore the gelatin causes approximately a threefold decrease in $\Delta\eta$. As mentioned in the discussion of the zero field viscosity, the gelatin surfactant layer acting as an electrosteric repulsion barrier decreases the attraction force between the agglomerates. As a consequence this hinders the particle structure formation, which results in a weaker response to magnetic field. With gelatin additive not just the zero field rheological properties, but also the magnetic response can be fine tuned and tailored to specific needs.

 https://doi.org/10.1016/j.heliyon.2019.e01507

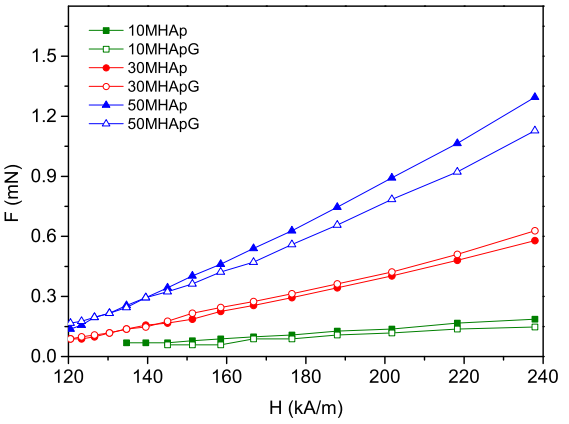

Figure 8. The magnetic field strength dependence of the magnetic body force acting on the droplets of the suspensions.

Time dependence

In the absence of a magnetic field the viscosity of the MHAp suspensions was decreasing over time at a constant shear rate, i.e. these samples showed thixotropic behavior. This is characteristic if the clusters are breaking up, and this process is not instantaneous. Regarding the gelatin containing MHApG suspensions no thixotropy could be observed, which is consistent with that there is no attractive particle network because of the gelatin surfactant layer.

In a magnetic field the viscosity of the MHAp suspensions showed strong time dependence. After the field was switched on, the viscosity increased continuously, indicating delayed agglomeration and structure formation despite the shearing. On the other hand, the viscosity of the MHApG suspensions reached the maximum $\Delta\eta$ in a much shorter time (~5 s) and after that it remained constant.

3.3.2. Inhomogeneous magnetic field

The results of the magnetic force measurements are shown in Figure 8. If the droplet is uniformly magnetized, then the body force depends on the V volume, the M magnetization of the sample, and the $\frac{dH_e}{dx}$ external magnetic field gradient as $F = VM\mu_0\frac{dH_e}{dx}$, where μ_0 is the permeability of vacuum [18]. As expected, with increasing magnetic field strength (and gradient) the force acting on the droplets is increasing for all composites. In the investigated field strength regime (H = 120-238 kA/m, with the corresponding gradient between 2821 and 22089 kA/m^2) the value of the measured force is in the order of 0.1-1 mN. Both the magnetite and gelatin content affects the magnetic force. At a given field strength the force is increasing with the Fe_3O_4 loading of the composites (Figure 9). This is caused by the increased magnetization of the samples at higher magnetite nanoparticle

 https://doi.org/10.1016/j.heliyon.2019.e01507

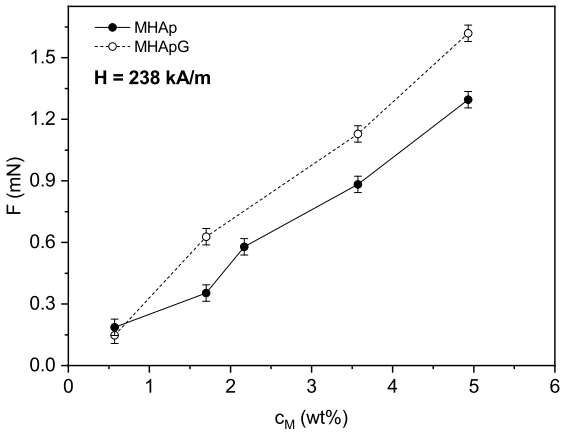

Figure 9. The force acting on the droplets of the suspensions as a function of the magnetite concentration in the case of MHAp (filled symbols) and MHApG (empty symbols) composites.

concentrations. As it can be seen in Figure 9 in the case of the gelatin containing MHApG composites the measured force is larger than the value expected from the magnetite concentration. The slightly increased magnetization of the MHApG composites can be attributed to the different particle size distribution due to the hindrance of agglomeration by gelatin. This is supported by the results of the susceptibility measurements also.

4. Conclusions

Magnetite/hydroxyapatite composites were synthesized and the response of their aqueous suspensions to homogeneous and inhomogeneous magnetic fields was investigated. We have demonstrated that the magnetite concentration and the gelatin content largely affect the rheological properties of the composites. The MHAp samples showed shear thinning, while the MHApG composites exhibited close to Newtonian behavior both in the absence and in the presence of a homogeneous magnetic field.

The addition of gelatin decreased the zero field viscosity by two orders of magnitude due to the formation of a surfactant layer and therefore obstructing the agglomeration of the particles. The zero field viscosity of the MHAp suspensions decreased significantly when the Fe_3O_4 concentration was larger.

The viscosity increment in magnetic field was increasing with the magnetite concentration, but the gelatin as a surfactant hindered the structure formation, resulting in a weaker response of the MHApG composites to magnetic field. Strong time dependence of the viscosity was observed for the MHAp suspensions. The zero field behavior was thixotropic, while in magnetic field the viscosity increased over time.

 https://doi.org/10.1016/j.heliyon.2019.e01507

The magnetic body force under inhomogeneous field increased with the magnetic field strength and the magnetite loading of the composites. The measured magnetic force was larger in the case of the MHApG composites due to the different particle size distribution.

In this study it was shown that the formulation of magnetic HAp composites could have a drastic effect on the magnetic response. With additives like gelatin the magnetic behavior and the rheological properties of magnetic HAp composites can be fine tuned and tailored to specific needs. We believe the better understanding of these aspects could help in the design and fabrication of new biomaterials.

Declarations

Author contribution statement

Barnabás Horváth: Conceived and designed the experiments; Performed the experiments; Analyzed and interpreted the data; Wrote the paper.

Melinda Rigó, Sándor Guba: Performed the experiments; Contributed reagents, materials, analysis tools or data.

István Szalai, Réka Barabás: Conceived and designed the experiments.

Funding statement

This work was supported by the BIONANO GINOP-2.3.2-15-2016-00017 project, and Széchenyi 2020 (EFOP-3.6.1-16-2016-00015).

Competing interest statement

The authors declare no conflict of interest.

Additional information

No additional information is available for this paper.

Acknowledgements

The authors wish to thank Prof. Dr. Etelka Tombácz and Dr. Ildikó Tóth (University of Szeged) for the preparation of the magnetite nanoparticles. We are grateful for the

help of the coworkers at the Institute of Materials Engineering and the Institute of Environmental Engineering (University of Pannonia).

References

[1] A.K. Gupta, M. Gupta, Synthesis and surface engineering of iron oxide nanoparticles for biomedical applications, Biomaterials 26 (2005) 3995–4021.

[2] Q.A. Pankhurst, J. Connolly, S.K. Jones, J. Dobson, Applications of magnetic nanoparticles in biomedicine, J. Phys. D, Appl. Phys. 36 (2003) R167–R181.

[3] M.T. Lopez-Lopez, G. Scionti, A.C. Oliveira, J.D.G. Duran, A. Campos, M. Alaminos, I.A. Rodriguez, Generation and characterization of novel magnetic field-responsive biomaterials, PLoS ONE (2015) e0133878.

[4] S.S. Syamchand, G. Sony, Multifunctional hydroxyapatite nanoparticles for drug delivery and multimodal molecular imaging, Mikrochim. Acta 182 (2015) 1567–1589.

[5] S. Mondal, P. Manivasagan, S. Bharathiraja, M.M. Santha Moorthy, V.T. Nguyen, H.H. Kim, S.Y. Nam, K.D. Lee, J. Oh, Hydroxyapatite coated iron oxide nanoparticles: a promising nanomaterial for magnetic hyperthermia cancer treatment, Nanomaterials 7 (2017).

[6] H. Yang, H. Zeng, L. Hao, N. Zhao, C. Du, H. Liao, Y. Wang, Effects of hydroxyapatite microparticle morphology on bone mesenchymal stem cell behavior, J. Phys. Chem. B 2 (2014) 4703–4710.

[7] S. Panseri, C. Cunha, T. D'Alessandro, M. Sandri, A. Russo, G. Giavaresi, M. Marcacci, C.T. Hung, A. Tampieri, Magnetic hydroxyapatite bone substitutes to enhance tissue regeneration: evaluation in vitro using osteoblast-like cells and in vivo in a bone defect, PLoS ONE 7 (2012) e38710.

[8] B. Govindan, B.S. Latha, P. Nagamony, F. Ahmed, M.A. Saifi, A.H. Harrath, S. Alwasel, L. Mansour, E.H. Alsharaeh, Designed synthesis of nanostructured magnetic hydroxyapatite based drug nanocarrier for anti-cancer drug delivery toward the treatment of human epidermoid carcinoma, Nanomaterials 7 (2017).

[9] S. Suarasan, M. Focsan, M. Potara, O. Soritau, A. Florea, D. Maniu, S. Astilean, Doxorubicin-incorporated nanotherapeutic delivery system based on gelatin-coated gold nanoparticles: formulation, drug release, and multimodal imaging of cellular internalization, ACS Appl. Mater. Interfaces 8 (2016) 22900–22913.

[10] S.C. Chao, M.J. Wang, N.S. Pai, S.K. Yen, Preparation and characterization of gelatin-hydroxyapatite composite microspheres for hard tissue repair, Mater. Sci. Eng., C 57 (2015) 113–122.

[11] Z. Wang, P. André, D. McLean, S.I. Brown, G.J. Florence, A. Cuschieri, Intraluminal magnetisation of bowel by ferromagnetic particles for retraction and manipulation by magnetic probes, Med. Eng. Phys. 36 (2014) 1521–1525.

[12] M. Maas, U. Hess, K. Rezwan, The contribution of rheology for designing hydroxyapatite biomaterials, Curr. Opin. Colloid Interface Sci. 19 (2014) 585–593.

[13] Y. Jiao, D. Gyawali, J.M. Stark, P. Akcora, P. Nair, R.T. Tran, J. Yang, A rheological study of biodegradable injectable PEGMC/HA composite scaffolds, Soft Matter 8 (2012) 1499–1507.

[14] S. Deb, J. Giri, S. Dasgupta, D. Datta, D. Bahadur, Synthesis and characterization of biocompatible hydroxyapatite coated ferrite, Bull. Mater. Sci. 26 (2003) 655–660.

[15] C.H. Hou, S.M. Hou, Y.S. Hsueh, J. Lin, H.C. Wu, F.H. Lin, The in vivo performance of biomagnetic hydroxyapatite nanoparticles in cancer hyperthermia therapy, Biomaterials 30 (2009) 3956–3960.

[16] J.Y. Huang, M.H. Chen, W.T. Kuo, Y.J. Sun, F.H. Lin, The characterization and evaluation of cisplatin-loaded magnetite–hydroxyapatite nanoparticles (mHAp/CDDP) as dual treatment of hyperthermia and chemotherapy for lung cancer therapy, Ceram. Int. 41 (2015) 2399–2410.

[17] I.Y. Tóth, E. Illés, R.A. Bauer, D. Nesztor, M. Szekeres, I. Zupkó, E. Tombácz, Designed polyelectrolyte shell on magnetite nanocore for dilution-resistant biocompatible magnetic fluids, Langmuir 28 (2012) 16638–16646.

[18] S. Guba, B. Horváth, I. Szalai, Determination of the force acting on biocompatible ferrofluid droplets in inhomogeneous magnetic field, J. Magn. Magn. Mater. 444 (2017) 173–177.

[19] N.C. Blumenthal, F. Betts, A.S. Posner, Formation and structure of Ca-deficient hydroxyapatite, Calcif. Tissue Int. 33 (1981) 111–117.

[20] L. Berzina-Cimdina, N. Borodajenko, Research of calcium phosphates using Fourier transform infrared spectroscopy, in: T. Theophanides (Ed.), Infrared Spectroscopy, Intech, Rijeka, 2012.

[21] Z.H. Cheng, A. Yasukawa, K. Kandori, T. Ishikawa, FTIR Study on incorporation of CO2 into calcium hydroxyapatite, J. Chem. Soc. Faraday Trans. 94 (1998) 1501–1505.

[22] B.C. Vidal, M.L. Mello, Collagen type I amide I band infrared spectroscopy, Micron 42 (2011) 283–289.

[23] M. Dardouri, J.P. Borges, A.D. Omrani, Tailoring the morphology of hydroxyapatite particles using a simple solvothermal route, Ceram. Int. 43 (2017) 3784–3791.

[24] S.P. Sun, M. Wei, J.R. Olson, M.T. Shaw, Rheological behavior of needle-like hydroxyapatite nano-particle suspensions, Rheol. Acta 50 (2011) 65–74.

[25] Y.P. Seo, Y. Seo, Modeling and analysis of electrorheological suspensions in shear flow, Langmuir 28 (2012) 3077–3084.

[26] C.N. Likos, K.A. Vaynberg, H. Löwen, N.J. Wagner, Colloidal stabilization by adsorbed gelatin, Langmuir 16 (2000) 4100–4108.